MULTISPECTRAL IMAGING APPLICATION FOR FOOD INSPECTION

Bosoon Park   Y. R. Chen[1]

ABSTRACT

A multispectral imaging system with selected wavelength optical filter was demonstrated feasible for food safety inspection. Intensified multispectral images of carcasses were obtained with visible/near-infrared optical filters (542 - 847 nm wavelengths) and analyzed. The analysis of textural features based on co-occurrence matrices was conducted to determine the feasibility of a multispectral image analyses for discriminating unwholesome poultry carcasses from wholesome carcasses. The mean angular second moment of the wholesome carcasses scanned at 542 nm wavelength was lower than that of septicemic ($P \leq 0.0005$) and cadaver ($P \leq 0.0005$) carcasses. On the other hand, for the carcasses scanned at 700 nm wavelength, the feature values of septicemic and cadaver carcasses were significantly ($P \leq 0.0005$) different from wholesome carcasses. The discriminant functions for classifying poultry carcasses into three classes (wholesome, septicemic, cadaver) were developed using linear and quadratic covariance matrix analysis method. The accuracy of the quadratic discriminant models, expressed in rates of correct classification, were over 90% for the classification of wholesome, septicemic, and cadaver carcasses when textural features from the spectral images scanned at the wavelength of 542 and 700 nm were utilized.

KEYWORDS: Machine vision, Image Processing, Poultry Inspection, Classification, Discriminant Analysis, Chicken, Septicemic, Cadaver

INTRODUCTION

Machine vision and image processing techniques are useful for agricultural and food industry applications, particularly in grading and inspection (Park and Chen 1994; Liao et al., 1992; Steinmetz et al., 1993; Ni et al., 1993), because the majority of inspection tasks are highly repetitive and extremely boring, and their effectiveness depends on the efficiency of the human inspector.

In industrial situations, inspection consists of measurement or comparison of spatial geometry with those of known patterns, i.e., spatial pattern recognition method. While spatial imaging resolves objects into their mophological dimensions, spectral imaging resolves a phenomenon of the interaction of light and objects to be inspected.

The multispectral images provided more information than the standard RGB color images, because they recover more information about the variation of the spectral reflectance of materials. The surface's texture and reflectances at specific wavelengths can be yielded and the sample's size and shape can be imaged and measured as well.

Image texture has been used in image analysis for segmentation and classification. Early studies for image texture analysis have involved autocorrelation functions (Liu et al., 1993), power spectra, and relative frequencies of various gray levels on the unnormalized image (Park and Chen, 1994). Gray-tone spatial-dependence matrix, so called co-occurrence matrix (COM),

---

[1] Bosoon Park and Y.R. Chen are Agricultural Engineer and Research Leader, respectively, of the Instrumentation and Sensing Laboratory, Beltsville Agricultural Research Center, Agricultural Research Service, U.S. Department of Agriculture, Beltsville, Maryland 20705-2350.

has been also used for image texture analysis for agricultural applications (Park et al., 1992; Shearer and Holmes, 1990).

Since the image texture contains statistical information of gray level image in the spatial domain, textural analysis may be able to classify agricultural commodities. Also, image texture analysis is useful because texture is independent of the tone of the image. Thus, image texture analysis is one of the most important processes in image analysis because it partitions an image into meaningful regions. However, there has been little research for analyzing performance of COM as a function of parameters such as angle and distance in agricultural product quality evaluation and safety inspection.

The primary goals of this study were 1) to examine the performance of cooccurrence matrix texture analysis method as a tool of multispectral image analysis for food inspection; 2) to develop the linear and/or nonlinear discriminant models for poultry carcass classification.

Multispectral Imaging

Spectral Imaging involves measuring the intensity of diffusely reflected light from a surface. The reflected light contains information about the absorbers near the surface of the material which modifies the reflection. By using wavelengths selected across a waveband, it is possible to construct a characteristic spectral features for the material (Muir, 1993). These spectral patterns or images are multi-dimensions and the process of distinguishing between them is called spectral pattern recognition.

The absorbing molecules of matter are excited to specific vibrational states or energy levels dependent on the energy of the incoming radiation. According to quantum theory, molecules absorb light in the visible and ultraviolet because their electrons can move to higher energy states. Infrared light does not have enough energy to excite electrons in molecules. Instead, excitations resulting in molecular absorption come from vibrations and rotations of molecules. Rotational absorption bands are predominantly in the far infrared. Vibrational absorption bands are those which involve the near infrared, which has been applied extensively to component analysis of food and agricultural materials. The complexity of molecular absorption can be simplified by assuming that molecules only vibrate at fixed frequencies when excited and so only absorb light of that particular frequency or associated wavelength (Muir et al., 1989).

Light which has interacted with a surface has penetrated just beneath the surface and been exposed to possible absorbers and then re-emitted from the surface. As such it contains information on the absorbers present in the material. By using a camera which can measure the intensity of diffusely reflected light at wavelengths across a waveband it is possible to obtain the characteristic spectral features of materials.

MATERIALS AND METHODS

Hardware

A multispectral camera (Model IMC-201, Xybion Electronic System)[2] containing six visible/near-infrared interference optical filters with wavelengths of 542, 570, 641, 700, 720, and 847 nm (each filter has 10 nm narrow bandwidth) was used. The multispectral camera had an dynamic aperture control capability at the different spectral bands, an enhanced calibration capability, and a sufficient sensitivity for using narrow band spectral filters to enhance

---

[2] Mention of any company or trade name is for identification only and does not imply endorsement by the U.S. Department of Agriculture.

measurement accuracy. The intensified CCD imager provides significantly increased sensitivity, which allows the use of narrow band spectral filters for better discrimination performance.

The camera had two on-board Motorola MC68HC11 microprocessors, a Sony XC-77 CCD imager with a 400-1000 nm spectral range. The imager was fiber-optically coupled to a microchannel plate (MCP) intensifier. A Tokina AT-X lens with a variable focal length of 28 to 85 mm was used. An IBM-compatible computer with an A/D converter was used for image capture and camera control via RS-232. The system computer was a Gateway 486 with a 50 MHz clock speed and an 8 bit image digitizer (ImCap, Xybion Electronic System, Cedar Knolls, NJ). Two high intensity halogen lamps (Tota T-110, Lowel-Light, Inc., Brooklyn, N.Y.) were used as the light source to provide 248 lux (lumen/m^2) of light on the object. A DC power supply (Nobatron DCR 150-5A, Raytheon Co., South Norwalk, Conn.) was used for regulating lamp power. A soft silver umbrella was attached to the each lamp for diffusing the light. The multispectral imaging system used in the study was reported more detail in a previous paper (Park and Chen, 1994).

Software

Image Processing Tools for Windows 95® software was developed at the Instrumentation and Sensing Laboratory. This software consists of two parts. The first part is for real-time image acquisition and the second part is for processing and analyzing spectral images. The software provides many basic image processing functions such as converting image format, cropping the region of interest (ROI) of the image, reading image size, enhancing linear contrast, resizing, generating image data for texture analysis, and analyses of multispectral images. The software utilized Microsoft C++ (Microsoft Co., Roselle, IL) compiler.

The size of an original spectral image captured by a camera was 786 x 493 (387,498 pixels). This image was reduced to a size of 254 x 240 (60,960 pixels). The intensity of each pixel was an average of 3 x 2 template of an original image. Finally, a 64 x 64 subimage was cropped from the reduced images. The image was first loaded into an active window, the ROI was then specified for further processing. The ROI image was then used for generating data ready for COM and displaying on the active window for further analysis.

Co-occurrence matrix of image texture

The co-occurrence matrix (COM) contains not only textural information but spectral information as well. Haralick et al. (1973) presented the general procedure for extracting textural properties of image data in the spatial domain. They computed a set of gray-tone spatial-dependence probability-distribution matrices for a given image and suggested a set of 14 textural features which can be extracted from each COM.

The gray-tone spatial-dependence matrix measures the probability that a pixel of a particular gray level will occur at an orientation and a specified distance from its neighboring pixels given that these pixels have a second particular gray level. COM is represented by the function $P(i,j,d,\theta)$, where i represents the gray level of location (x,y), and j represents the gray level of its neighbor pixel at a distance d and an orientation of θ from location (x,y). The eight nearest neighbor resolution cells (3 x 3 matrix), where the surrounding resolution cells were expressed in terms of their spatial orientation to the central reference pixel (i,j). The eight neighbors represent all image pixels at a distance of 1. Resolution cells (i+1,j) and (i-1,j) are nearest-neighbors to the reference cell (i,j) in the horizontal direction ($\theta = 0°$) and at a distance, d=1. This concept can be extended to the three additional orientations ($\theta = 45°, 90°,$ and $135°$).

The COM is scale invariant, i.e., the matrices would be the same if all pixels of certain gray level in image matrix were changed to other constant value. These matrices show the

relative frequency distributions of gray levels and describe how often one gray level will appear in a specified spatial relationship to another gray level on each image region. Because there are eight nearest neighbors for each pixel, there exist many different co-occurrence matrices from the same gray-tone image based on direction and distance from the reference cell for each image region. In this study, the textural features were calculated from the co-occurrence matrix when $\theta=0°, 45°, 90°, 135°$ and $d=1, 2$. For more detail about COM, see Park and Chen (1996).

Textural features

Angular Second Moment (f_1) is a measure of homogeneity of the image and can be calculated from the normalized COM. The higher value of this feature means that the amplitude or intensity changes less in the image and results in a co-occurrence matrix is much sparser.

Contrast (f_2) measures local variation in the image. Higher contrast value indicates high amount of local variation. Correlation (f_3) is a measure of linear dependency of intensity values of an image. For an image with large areas of similar intensities, correlation will be much higher than for an image with noisier, uncorrelated intensities (Shearer and Holmes, 1990). Variance (f_4) indicates the variation of values of image intensity. For an image whose all pixels have the same intensity, the variance would be zero. The inverse difference moment (f_5) was used as an another feature of image contrast.

Other textural features calculated for this research were sum average (f_6), sum variance (f_7), sum entropy (f_8), entropy (f_9), difference variance (f_{10}), and difference entropy (f_{11}). Sum average and sum variance are the average and variance of normalized gray-tone image in the spatial domain, respectively. The sum entropy is a measure of randomness within an image and entropy is an indication of the complexity within an image. The more complex an image, the higher entropy value. The difference variance is an image variation in a normalized gray-tone spatial-dependence matrix. The difference entropy is also an indication of the amount of randomness in an image.

Discriminant Analysis

The discriminant analysis can be useful to find a discriminant function for guessing to which class an observation belongs, based on knowledge of the quantitative variables and a set of linear combinations of the quantitative variables. Linear or quadratic discriminant functions can be used for data with approximately multivariate normal within-class distributions. The performance of a discriminant function can be evaluated by estimating error rates (probabilities of misclassification). The error rates can also be estimated by cross-validation.

Discriminant functions classify observations into two or more groups on the basis of one or more quantitative variables. When the distribution within each group is assumed to be multivariate normal, a parametric method can be used to derive a linear or quadratic discriminant function. The discriminant function is determined by a measure of generalized squared distance. The classification criterion can be based on either the individual within-group covariance matrices (quadratic function) or the pooled covariance matrix (linear function). Each observation is placed in the class from which it has the smallest generalized squared distance. This method also computes the posterior probability of an observation belonging to each class.

The squared distance from x to group t is

$$d_t^2(x) = (x - m_t)' V_t^{-1}(x - m_t)$$

where, x = p-dimensional vector containing the quantitative variables of an observation, t = subscript to distinguish the groups, $V_t = S_t$ for quadratic model, or $V_t = S$ for linear model; S_t = covariance matrix within group t, S = pooled covariance matrix

The probability of x belonging to group t, by using Bayes' theorem:

$$p(t|x) = q_t f_t(x) / f(x)$$

where, $f_t(x)$ is the group-specific density estimate at x from group t, and $f(x) = \sum_t q_t f_t(x)$ is the estimated unconditional density at x.

The group-specific density estimate at x from group t is then given by

$$f_t(x) = (2\pi)^{-p/2} |V_t|^{-1/2} \exp\left(-0.5d_t^2(x)\right)$$

Using Bayes' theorem, the posterior probability of x belonging to group t is

$$p(t|x) = \frac{q_t f_t(x)}{\sum_u q_u f_u(x)}$$

The generalized squared distance from x to group t is defined as

$$D_t^2(x) = d_t^2(x) + g_1(t) + g_2(t)$$

where,

$g_1(t) = \log_e|S_t|$ for quadratic model, or $g_1(t) = 0$ for linear model; and $g_2(t) = -2\log_e(q_t)$ if the prior probabilities are not all equal, or $g_2(t) = 0$ if the prior probabilities are all equal

The posterior probability of x belonging to group t is then equal to

$$p(t|x) = \frac{\exp\left(-0.5D_t^2(x)\right)}{\sum_u \exp\left(-0.5D_u^2(x)\right)}$$

An observation is classified into group u if setting $t = u$ produces the largest value of $p(t|x)$ or the smallest value of $D_t^2(x)$.

Application for Poultry Inspection System

A total of 142 chicken carcasses, 44 wholesome, 40 septicemia, and 58 cadaver, were obtained from poultry processing plants on Maryland's Eastern Shore and West Virginia in January and July, 1993, respectively. The conditions of these carcasses were identified by the USDA Food Safety and Inspection Service (FSIS) veterinarians on the plant site. The carcasses were separated based on the condition of condemnation and placed in plastic bags to minimize dehydration. Then the bags were placed in the coolers filled with ice and transported to the

Instrumentation and Sensing Laboratory located at Beltsville, Maryland to perform the multispectral image measurement. At the laboratory the chickens were stored in a 0 °C cold room for 15 hours prior to the experiments.

Procedure

Chicken carcasses were hung on a shackle. Diffused light from a pair of tungsten halogen lamps was projected on the carcasses. Images of the carcasses were taken using the multispectral camera. The total response of a multispectral imaging subsystem is the function of illuminator power, filter characteristics, sample reflectance, and detector sensitivity. These relationships vary with wavelength, therefore, these factors were carefully considered when the imaging subsystem was set up for experiments.

A white Teflon^{TM} block was used as a reference for the calibration of the imaging system because of its flat spectral reflectivity across the entire spectrum under the scan. The lens aperture was set at f/8 and the gain of the intensifier was set at 70% of the maximum gain for acquiring high quality images and also to prevent the over saturation of the images at the 641 nm wavelength band.

Six multispectral images, one image per each filter, were captured from each chicken, yielding a total of 852 images, for respectively 264 wholesome, 240 septicemic, and 348 cadaver, spectral images were captured from the 142 chicken carcasses. All digitized image data were converted into a bitmap format for image processing and analysis.

The chicken images were processed for gray-tone spatial-dependence matrix image textural analysis. First of all the image captured using the wavelength of 641 nm filter was utilized as the template for the segmentation of the object because this image had high intensity contrast to the background. The chicken objects in a segmented image scanned by other filters were identified for image feature measurement. All pixels of the objects were digitized (0 - 255) for the calculation of gray values. In order to obtain the image textural features, the co-occurrence matrices were generated from the gray-tone images.

RESULTS AND DISCUSSION

Variability of COM textural feature

Textural features varied with the distance and angle of COM as well as condemnation of poultry carcasses. Textural features between wholesome and unwholesome carcasses were compared based on the statistical significance tests. Feature values of the wholesome carcasses scanned at 542 nm wavelength were significantly different from those of septicemic (P ≤ 0.0005) and cadaver (P ≤ 0.0005) carcasses, but no significant difference existed between septicemic and cadaver carcasses when the COM of distance equals 1 and angle equals 0 were compared. However, the textural features of septicemic carcass (d = 1 and θ = 0°) were significantly (P ≤ 0.01) different from those of cadaver carcass (d = 2 and θ = 0°). The feature values of septicemic and cadaver carcasses were significantly (P ≤ 0.0005) different from the features of wholesome carcass when distances equal 1 and 2, the angles equal 0°, 45°, 90°, and 135°, respectively. Within same carcass groups, the textural feature values at θ = 0° were much higher (P ≤ 0.0005) than the feature values at θ = 45°, 90°, and 135°. For the carcasses scanned at 700 nm wavelength, the feature values of septicemic and cadaver carcasses (d = 1 and θ = 0°) were significantly (P ≤ 0.0005) different from the feature values of wholesome carcasses (d = 2 and θ = 45°, 90°, and 135°). While, no significant difference was found between septicemic and cadaver carcasses (d = 1 and θ = 0°).

Figure 1 compared the feature values of mean angular second moment of different carcasses scanned at 542 and 700 nm wavelengths as a function of distance and angle for generating COM. Angular second moment of the wholesome carcasses scanned at 542 nm wavelength was lower than that of septicemic (P ≤ 0.0005) and cadaver (P ≤ 0.0005) carcasses, but no significant difference existed between septicemic and cadaver carcasses when the COM of distance equals 1 or 2 and angle equals 0°, 45°, 90°, and 135° were compared. Similarly, the mean value of angular second moment of wholesome carcasses scanned at 700 nm wavelength was lower than that of septicemic (P ≤ 0.05) and cadaver (P ≤ 0.05) carcasses. In this case, the value of septicemic carcass was higher than that of cadaver carcass for all different parameters (d = 1 and 2; θ = 0°, 45°, 90°, and 135°). As shown in figure, the mean angular second moment values of wholesome, septicemic and cadaver carcass (d = 1 and θ = 0°) was much higher (P ≤ 0.0005) than those values with θ = 45°, 90°, and 135° when distance equals 2. Thus, the textural feature values of spectral images changed with the parameters, specifically distance and angle for generating COM.

Accuracy of discriminant model

Discriminant functions were developed for separation of the septicemic and cadaver from the wholesome carcasses using discriminant analysis of selected wavelengths. Table 1 shows the accuracy of discriminant models for classifying wholesome and unwholesome, in this case septicemic and cadaver, poultry carcasses.

The accuracy of the discriminant models for calibration varied with not only the parameters for generating COM, but linearity of models as well. For the poultry inspection application, quadratic discriminant models were selected because the separation accuracy of all three cases, wholesome, septicemic, and cadaver, was high enough to compare to other models. In this case, the angle for generating COM was 0° at the wavelengths of 542 and 700 nm.

The accuracy for calibration quadratic models varied from 90.9% to 95.8% when textural features of spectral image at 542 nm wavelength were used as inputs. For the separation of wholesome carcasses, the accuracy of model was 90.9% for calibration and 100% for test. Similarly, the accuracy of discriminant modes were 95.8% for calibration and 90% for test for the separation of septicemic carcasses. While, for the separation of cadaver carcasses, the input features of spectral image at 700 nm wavelength was useful for model development. In this case, the accuracy of discriminant model was 93.3% for calibration and 90% for test, respectively.

CONCLUSIONS

This study was conducted to determine the feasibility of a multispectral imaging system for food inspection. Six visible/NIR wavelengths, 542, 571, 641, 700, 720, and 847 nm, were used for the poultry carcass inspection application. Co-occurrence matrix textural features of spectral images at the selected wavelengths were used for separation of unwholesome carcasses.

The analysis of textural features based on co-occurrence matrices was conducted. The mean angular second moment of the wholesome carcasses scanned at 542 nm wavelength was lower than that of septicemic (P ≤ 0.0005) and cadaver (P ≤ 0.0005) carcasses. Also, for the carcasses scanned at 700 nm wavelength, the feature values of septicemic and cadaver carcasses were significantly (P ≤ 0.0005) different from the feature values of wholesome carcasses.

The discriminant functions for classifying poultry carcasses into three classes (wholesome, septicemic, cadaver), were developed using linear and quadratic covariance matrix analysis method utilizing the COM image textural features at the selected wavelengths. The

results showed that the separation of wholesome carcasses from septicemic and cadaver carcasses performed with high classification accuracy.

The accuracy of the quadratic discriminant models, expressed in rates of correct classification, were 100% for wholesome, 90% for septicemic, and 90% for cadaver carcasses when textural features of COM generated from the spectral images scanned at the wavelength of 542 and 700 nm. Since textural features of spectral images varied with the parameters such as distance and angle for generating COM, the selection of optimum parameter values considering wavelength is the most important task to apply multispectral imaging technology for food inspection. Further textural feature analysis and discriminant model selection utilizing optimum parameters will be conducted for improving the classification accuracy of poultry carcasses.

ACKNOWLEDGMENTS

REFERENCES

1. Chen, Y. R., R. W. Huffman, and B. Park. 1993. Visible/NIR spectrophotometry for monitoring shelf life of chicken carcasses. ASAE Paper No. 936067, American Society of Agricultural Engineers. St. Joseph, MI.
2. Haralick, R.M., K. Shanmugam and I. Dinstein. 1973. Textural features for image classification. *IEEE Transactions on Systems, Man, and Cybernetics* SMC-3(6): 610-621
3. Liu, Y., D.J. Aneshansley, and J.R. Stouffer. 1993. Autocorrelation of ultrasound speckle and its relationship to beef marbling. *Transactions of the ASAE* 36(3): 971-977
4. Muir, A. Y., I. D. G. Shirlaw, and D. C. McRae. 1989. Machine vision using spectral imaging techniques. *Agricultural Engineer* 44(3): 79-81
5. Muir, A. Y. 1993. Machine vision and spectral imaging. *Agricultural Engineer* 48(4): 124
6. Ni, B., M. R. Paulsen, K. Liao, and J. F. Reid. 1993. An automated corn kernel inspection system using machine vision. ASAE Paper 933032. American Society of Agricultural Engineers. St. Joseph, MI.
7. Park, B., B.R. Thane, and A.D. Whittaker. 1992. Ultrasonic image analysis for beef tenderness. Optics in Agriculture and Forestry. SPIE Vol. 1836: 120-131
8. Park, B. and Y.R. Chen. 1994. Intensified multispectral image processing for poultry carcasses inspection. Proceedings of the Food Processing Automation Conference III, Orlando, FL: 97-106.
9. Park, B. and Y.R. Chen. 1996. Multispectral image co-occurrence matrix analysis for poultry carcasses inspection. *Transactions of the ASAE* 39 (in press)
10. Shearer, S.A. and R.G. Holmes. 1990. Plant identification using color co-occurrence matrices. *Transactions of the ASAE* 33(6): 2037-2044.
11. Steinmetz, V., M J. Delwiche, D. K. Giles, and R. Evans. 1993. Grading roses with machine vision. ASAE Paper 936070. American Society of Agricultural Engineers. St. Joseph, MI.
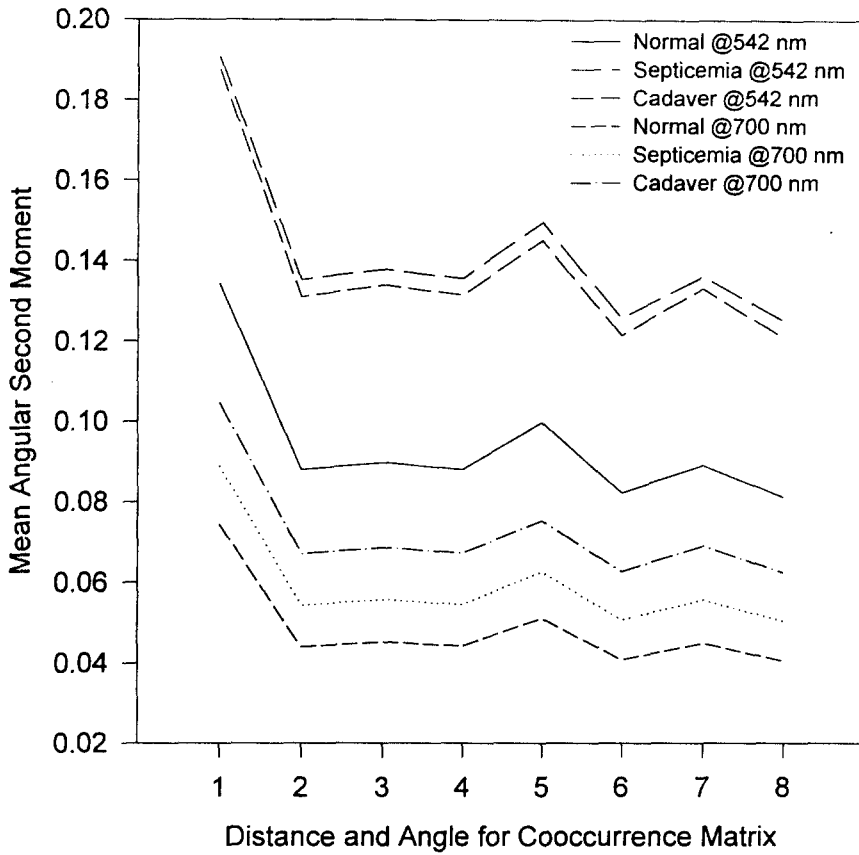
Figure 1. Mean angular second moment at different distance (D) and angle (θ) for generating cooccurrence matrix. Note: the number of x-axis means 1. D=1 and θ = 0°; 2. D=1 and θ = 45°; 3. D=1 and θ = 90°; 4. D=1 and θ = 135°; 5. D=2 and θ = 0°; 6. D=2 and θ = 45°; 7. D=2 and θ = 90°; 8. D=2 and θ = 135°

TABLE 1. Classification accuracy of wholesome, septicemic, and cadaver carcasses through statistical discriminant algorithm using cooccurrence matrix textural data with 0°, 45°, 90°, and 135° orientation and distance equal to 2.

Wave-length (nm)	CLS	Calibration								Test							
		Linear				Quadratic				Linear				Quadratic			
		0°	45°	90°	135°	0°	45°	90°	135°	0°	45°	90°	135°	0°	45°	90°	135°
542	N	60.6	66.7	66.7	66.7	90.9	90.9	87.9	84.9	90	100	100	100	100	100	100	100
	S	46.7	46.7	40.0	46.7	30.0	33.3	36.7	33.3	20	20	20	40	10	0	10	0
	C	89.6	91.7	97.9	87.5	95.8	95.8	97.9	95.8	60	80	80	70	90	90	80	90
570	N	60.6	66.7	66.7	63.6	90.9	90.9	93.9	90.9	90	90	90	90	90	10	90	90
	S	53.6	42.9	50.0	39.3	42.9	46.4	46.4	53.6	20	20	30	20	20	0	10	10
	C	87.5	89.6	85.4	85.4	91.7	93.8	95.8	93.8	90	80	100	90	90	90	90	80
641	N	75.0	68.8	71.9	78.1	87.5	90.6	84.4	90.6	80	90	80	80	40	70	80	70
	S	29.6	40.7	40.7	29.6	62.7	55.6	66.7	63.0	20	60	30	50	20	30	30	10
	C	80.0	86.0	82.0	84.0	88.0	90.0	92.0	90.0	80	100	90	90	90	100	90	100
700	N	76.5	61.8	64.7	55.9	88.2	91.2	97.1	85.3	60	70	70	70	70	70	50	60
	S	53.3	60.0	53.3	63.3	93.3	93.3	90.0	90.0	40	50	70	50	90	80	80	80
	C	85.4	83.3	72.9	85.4	66.7	72.9	62.5	79.2	100	100	100	81.8	50	90	90	72.7
720	N	55.9	58.8	61.8	58.8	88.2	85.3	91.2	88.2	60	60	30	50	60	60	50	60
	S	40.0	33.3	43.3	43.3	93.3	86.7	90.0	83.3	60	20	40	40	80	50	80	50
	C	75.0	75.0	68.8	72.9	56.3	79.2	66.7	77.1	100	100	100	100	60	80	70	70
847	N	64.7	50.0	55.9	58.8	73.5	61.8	50.0	52.9	60	60	70	60	30	40	30	30
	S	43.3	36.7	46.7	43.3	53.3	66.7	80.0	53.3	30	20	40	50	40	50	80	50
	C	79.2	77.1	77.1	83.3	85.4	91.7	75.0	85.4	70	60	70	60	90	100	80	100

Note: Sample numbers are calibration and validation (n=112) and test (n=30). Individual sample numbers were wholesome (n=44), septicemic (n=40), and cadaver (n=58), respectively. Cross-validation method was used for validation of the models.